Retained Austenite as a Hydrogen Trap in Steel Welds

Hydrogen trapping is investigated as a means of improving resistance to hydrogen-assisted cracking in HSLA steels

BY Y. D. PARK, I. S. MAROEF, A. LANDAU, AND D. L. OLSON

ABSTRACT. The role of retained austenite in hydrogen management of high-strength steel weld deposits was investigated. Retained austenite was found to be an intraphase hydrogen trapping site that has relatively high binding energy. To identify retained austenite as an intraphase hydrogen trapping site, four samples with different austenite volume fractions were prepared: AISI type 304 stainless steel, super duplex stainless steel, dual-phase steel (12 vol-% retained austenite), high-strength low-alloy (HSLA) steel weld deposit (4 vol-% and 0 vol-% retained austenite). Each of the samples was charged with 99.9% pure hydrogen by using gaseous charging. The thermal desorption analysis was employed to observe hydrogen trapping and detrapping behavior. Retained austenite is not only a diffusion-controlled trap, but also a metastable phase. The dual-phase steel (12 vol-% retained austenite) was investigated to observe the effects of applied plastic strain and reduced temperature by using thermal desorption analysis. When the plastic strain and reduced temperature were applied on hydrogen-charged specimens, the thermal desorption analysis exhibited a shifting of hydrogen peak to lower temperature. This result suggests microstructural transformation associated with changes in service conditions may result in a high diffusible hydrogen content in the resulting martensite phase, which is known as the most susceptible microstructure to hydrogen-assisted cracking (HAC). Demonstration of the hydrogen trapping capacity and the metastability of retained austenite suggests the amount of allowable retained austenite needs to be related to the amount of hydrogen pickup and the expected service condition.

Y. D. PARK, I. S. MAROEF, and D. L. OLSON are with the Center for Welding, Joining, and Coating Research, Colorado School of Mines, Golden, Colo. A. LANDAU is with Ben Gurion University of the Negev, Beer-Sheva, Israel.

Introduction

High-strength low-alloy (HSLA) steels are known to be susceptible to hydrogen cracking. As the strength is increased, so is the risk of hydrogen-assisted cracking (HAC) after welding. Hydrogen-assisted cracking in HSLA steel welds is considered to take place when all necessary conditions for cracking are simultaneously satisfied. These conditions include the combination of unacceptable diffusible hydrogen content, high restraint tensile stress, high hardness or a susceptible microstructure, and a temperature ranging between –100 and 100°C (Refs. 1, 2). The main goal to make a HAC-resisting, high-strength steel weldment is to reduce the amount of diffusible hydrogen. A common practice to reduce cold cracking in high-strength steel welding is with pre- or postweld heat treatment. Heat treatment is performed to reduce hardness and to ensure sufficient time for reduction of hydrogen from the weld.

Recently, the feasibility of a hydrogen trapping concept to improve HAC resistance on welding was investigated (Ref. 3). Hydrogen was found not only in the host lattice, but also segregated to atomic and microstructural defects such as vacancies, dislocations, grain boundaries, microvoids, and second-phase particles. In these localized regions, the mean residence time of a hydrogen atom was considerably longer than in a normal interstitial lattice site. This phenomenon is known as hydrogen trapping and these localized defect regions are hydrogen trapping sites (Ref. 4). The ability of a trap site to hold a hydrogen atom is associated with hydrogen trap binding energy.

Extensive investigations have been conducted on the crucial role of microstructure in hydrogen-assisted cracking in HSLA steel weld deposits (Ref. 5). It has been suggested that martensitic microstructure is most susceptible in hydrogen-assisted cracking in a weld deposit. However, the effect of retained austenite (or M/A constituent) on hydrogen-assisted cracking has not been studied. A certain amount of retained austenite is inevitable in HSLA steel weld deposits because of the thermal cooling cycle of welding. The resulting retained austenite exhibits a low hydrogen diffusivity and high hydrogen solubility. However, the surrounding microstructure of a HSLA weld deposit, which is a mixture of ferrite, martensite, and bainite, has high hydrogen diffusivity and low hydrogen solubility. These differences in hydrogen transport behavior between retained austenite and martensitic microstructure may result in retained austenite becoming a strong intraphase hydrogen trap, either temporarily or permanently. Nelson (Ref. 6) suggested that retained austenite can potentially be a continual hydrogen source to a martensitic matrix through its lifetime. Hence, an understanding of the role of retained austenite on HAC is necessary to design hydrogen-cracking-resisting HSLA steel weldments and to develop welding practices.

KEY WORDS

High-Strength Low-Alloy Steel
HSLA
Hydrogen-Assisted Cracking
HAC
Hydrogen Trapping
Retained Austenite
Thermal Desorption Analysis
Retained Austenite Stability

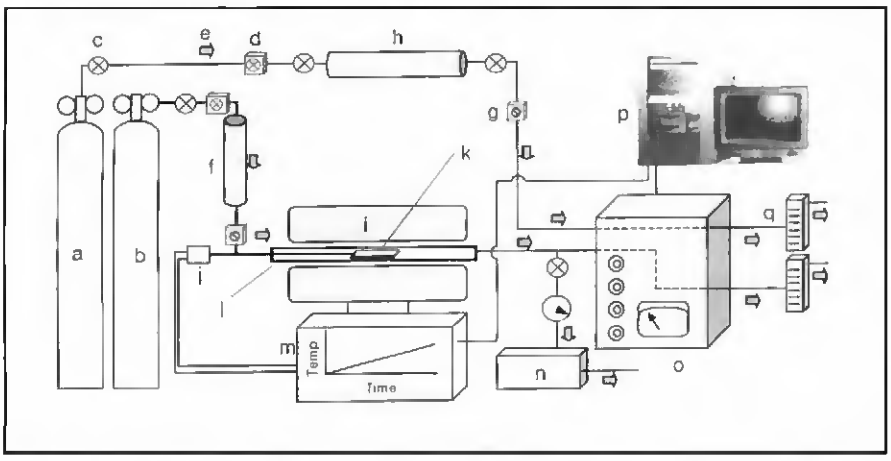

Fig. 1 — Hydrogen thermal desorption analysis apparatus. a — reference gas cylinder (argon); b — carrier gas cylinder (argon); c — valve; d — pressure gauge; e — gas flow direction; f — oxygen trap; g — flow gauge; h — moisture trap; i — furnace; j — thermocouple; k — sample; l — fused silica tube; m — furnace controller; n — vacuum pump; o — gas chromatograph; p — computerized data acquisition system; q — flow meter.

Furthermore, retained austenite is an unstable microstructure and may transform into martensite with changes in service temperature and applied plastic strain. In this event, hydrogen previously trapped in retained austenite may result in a very high diffusible hydrogen content injected into the adjacent martensitic microstructure.

Objectives

The first objective of this research was to evaluate retained austenite as a trap site and understand the potential role of retained austenite in hydrogen cracking in high-strength steel welds.

The second purpose was to establish the relationship between the stability of retained austenite and the altered hydrogen transport behavior after applying plastic strain and reduced service temperature.

Experimental Approach

Materials

Four different types of specimens for thermal desorption analysis were prepared: wrought AISI type 304 stainless steels (100 vol-% austenite phase), wrought super duplex stainless steels (50 vol-% austenite phase), intercritically heat-treated dual-phase steel (12 vol-% retained austenite), and HSLA steel weld deposits (4 and 0 vol-% retained austenite, respectively). The chemical compositions of consumables for shielded metal arc (SMA) welding of HSLA 100 steel were 1.2 wt-% manganese and 2.5 wt-% nickel. Other alloying additions were 0.5 wt-% molybdenum, 0.3 wt-% silicon, copper and chromium to lowest achievable levels, 0.06 max. wt-% carbon, 240 to 400 ppm titanium, and a goal of nitrogen below 100 ppm. Test welds were prepared in accordance with ISO 2560 using heat input of 51.2 kJ/in. and preheat of 149°C.

These materials were selected to achieve a matrix of materials with different amounts of austenite or retained austenite in the steels. The chemical compositions of samples are shown in Table 1. Each specimen was cut to the dimensions of 70 x 10 x 3 mm prior to hydrogen charging.

A commercial grade of AISI type 304 stainless steel was used. The super duplex stainless steel (SAF2507) was supplied by AB Sandvik. The dual-phase steels, which were cold-rolled sheet steel, were isothermally transformed at the intercritical annealing temperature (440°C) to produce about 12 vol-% retained austenite. The isothermally heated specimen was then oil-quenched to room temperature. Two types of HSLA steel weld deposits were prepared by multiple-pass shielded metal arc welding (SMAW). One type was cooled in air (4 vol-% retained austenite), and the other was quenched in liquid nitrogen (0 vol-% retained austenite). To achieve a smooth surface condition for the thermal desorption analysis, all samples were mechanically ground on a 1000-grit emery paper and followed by a 0.5-μm alumina polish.

To charge the hydrogen into the samples, a gaseous hydrogen charging system was used. The specimens were inserted in a sealed stainless steel canister, which was then evacuated and purged with a high flow of argon gas. Further, 99.9% pure gaseous hydrogen was purged into the sealed stainless steel canister, replacing the argon. The purging was done at two liters per minute flow rate and for as long as ten minutes. There was a possibility of incomplete replacement of argon by hydrogen, which would affect the amount of trapped hydrogen at the austenite phase. A consistent purging was exercised on every sample to allow for a fair comparison of one data to another. The final pressure of the canister was one atm. The stainless steel canister was placed into a furnace at 130°C for 24 h. Finally, hydrogen-charged samples were removed from the furnace, cooled in air, and placed in a dry condition for 24 h to remove any diffusible hydrogen from samples.

Thermal Desorption Analysis

The thermal desorption analytical technique measured the release of hydrogen from various trap sites during a constant rate heating of the samples. The methodology applied in this analysis provides an easy way to evaluate a specific trap without excessive interference from other traps coexisting in the samples. The analytical apparatus (Fig. 1) comprises a temperature-controlled furnace and a

Table 1 — Chemical Composition of Each Sample for Thermal Analysis (wt-%)

	C	Mn	P	Si	Cr	Ni	Mo	Cu	Al	V	N	Ti	O
AISI Type 304 Stainless Steels	0.08	2.0	0.03	0.42	19	8	0.49	—	—	—	—	—	
Super Duplex Stainless Steels	0.013	0.44	—	0.29	24.72	6.95	3.09	0.26	0.029	—	0.26	—	
Dual Phase Steel	0.138	1.57	0.006	1.126	—	<0.01	<0.005	—	0.027	—	0.004	—	
HSLA Weld Deposit	0.063	0.94	0.01	0.23	0.04	2.92	0.49	0.065	—	0.010	—	330 ppm	260 ppm

fused silica tube wherein the weld sample is heated at constant rate heating and under constant argon carrier flow. The optimum argon flow through the fused silica tube was found to be 10 mL/min. For the sample thickness of 3 mm used in this study, the flow rate was fast enough for separation of hydrogen evolution curves, but also slow enough to allow for sensitive detection by thermal conductivity detectors (TCD). The sample gas (argon and hydrogen) was fed into a gas chromatograph for quantitative analysis.

In the gas chromatograph, the gas sample entered the TCD. This detector produced a millivolt range output signal when a sample gas, with a different thermal conductivity than the carrier gas, passed through. Samples were heated with a constant heating rate (4°C/min) for trap identification.

The temperature dependency of hydrogen occupation at trap site follows the Fermi-Dirac statistics. Upon heating, hydrogen will be released from the trap sites at a rate dictated by the derivative of the occupation of trapped hydrogen with temperature. This derivative, which is the hydrogen evolution, takes place in a form of a Gaussian-like peak. The desorption rate of hydrogen from a weak trap will have a peak at a lower temperature than that of a strong trap. Further, the hydrogen thermal desorption analysis was used to assess the trapping parameters of retained austenite. The change in heating rate from 2 to 4°C/min is applied to calculate hydrogen binding energy, which will be explained more at Kissenger's analysis.

Optical, SEM, TEM Microscopy, and X-Ray Analysis

Specimens for optical microscopy were prepared by mechanical polishing through 0.05-μm alumina. Super duplex stainless steels were electrolytically etched for 5 to 20 s with 10% oxalic acid. LePera's reagent (Refs. 7, 8) was used to etch the HSLA steel weld deposits for optical microscopy. This etching method is based on sodium metabisulfite mixed with picric acid. The retained austenite and untempered martensite (or MA constituent) was identified with contrast enhancement resulting from LePera's reagent, which was a fresh solution of 4% picric acid in ethanol mixed with a 1% solution of sodium metabisulfite in distilled water in a 1:2 volume ratio.

Foil specimens for transmission electron microscopy (TEM) were first mechanically thinned by wet grinding to approximately 0.06 mm. Discs 3.0 mm in diameter were punched from the 0.06-mm wafer and were jet polished at room temperature for perforation in a Fischione twin-jet electropolisher with an electrolyte of 5 vol-%. Perchloric acid and 95 vol-% acetic were used with an applied current of 80 mA and 8 V. The thin foils were examined in a Philips EM400 with an accelerating voltage of 120 kV. Energy dispersive spectroscopy (EDS) analysis for retained austenite phase of HSLA steel weld deposit was carried out with a Philips CM200 scanning transmission electron microscopy (STEM) with an acceleration voltage of 200 kV.

X-ray diffraction (XRD) technique

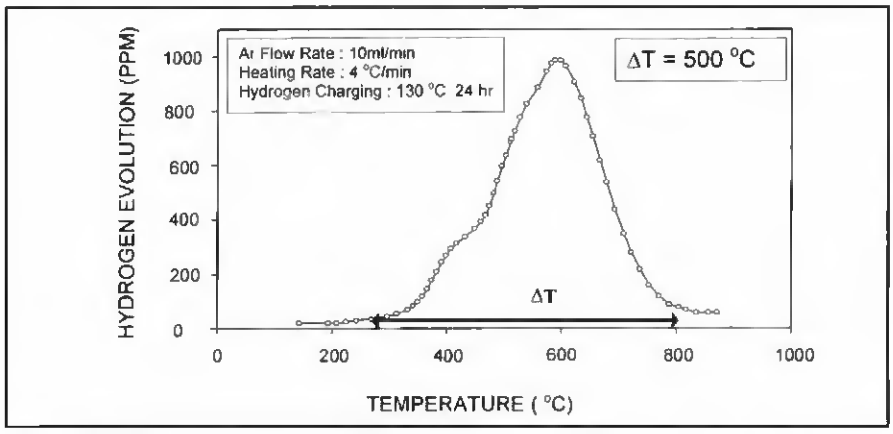

Fig. 2 — Typical thermal desorption analysis result from a hydrogen-charged AISI type 304 stainless steel sample.

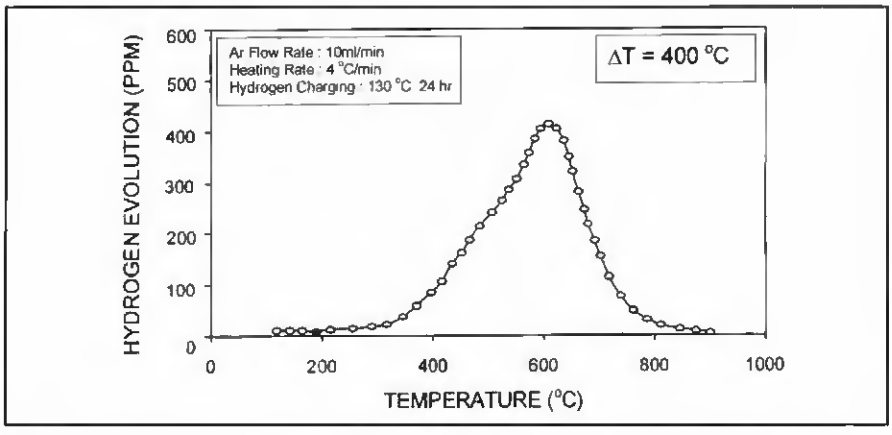

Fig. 3 — Thermal desorption analysis of hydrogen-charged super duplex stainless steel sample.

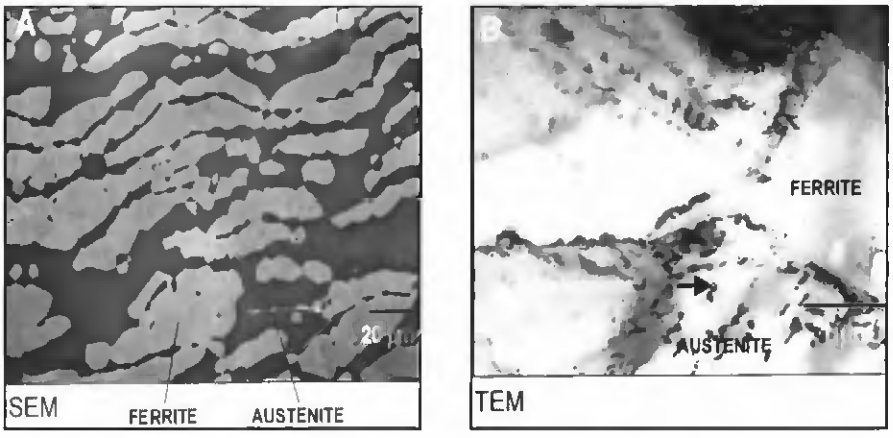

Fig. 4 — Microstructure of super duplex stainless steel. A — SEM; B — TEM.

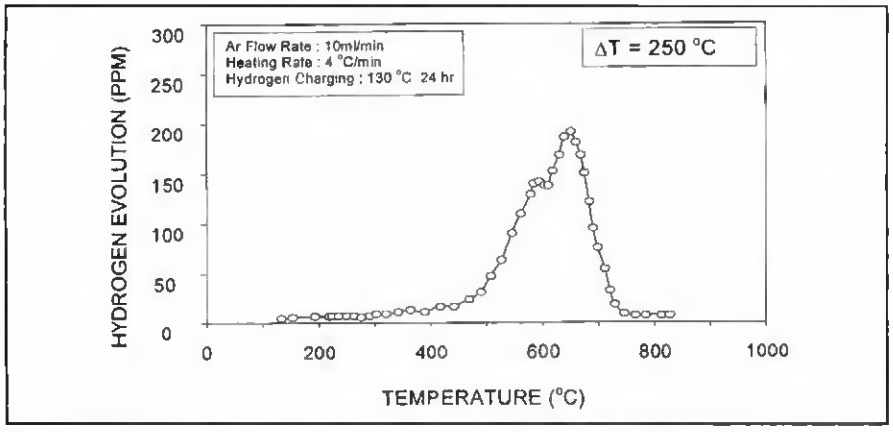

Fig. 5 — Thermal desorption analysis of a hydrogen-charged dual-phase steel sample.

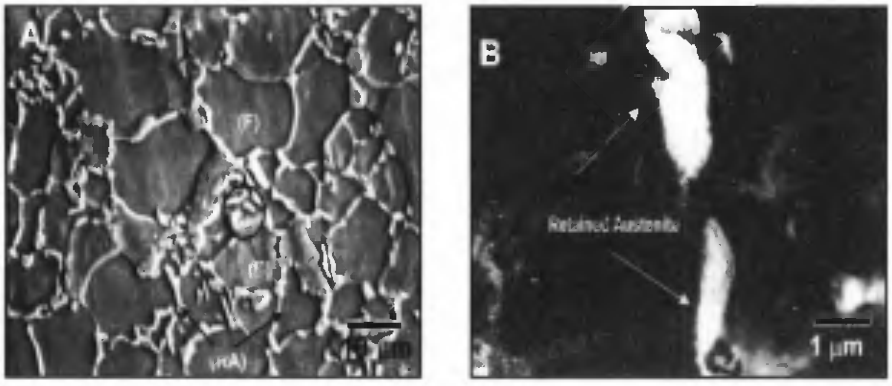

Fig. 6 — A — SEM microstructure of intercritically heat treated steel, which contains 12 vol-% retained austenite; B — detail of the area shown in A; (RA) Retained Austenite, (F) Ferrite, (B) Bainite.

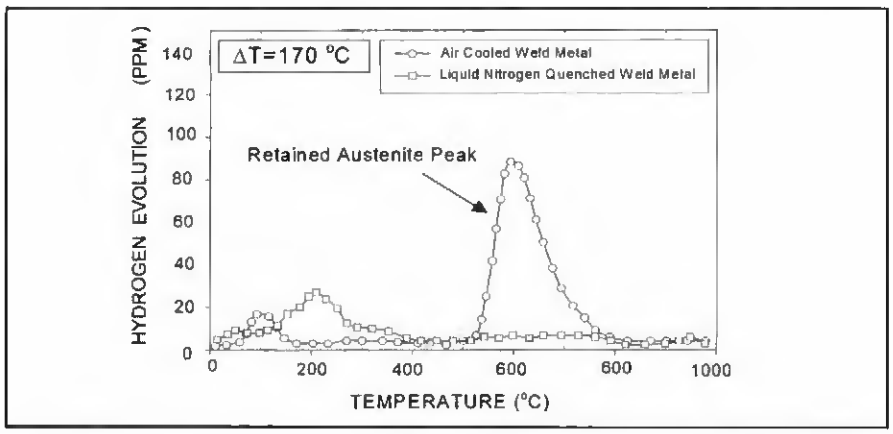

Fig. 7 — Thermal desorption analysis of hydrogen-charged HSLA steel weld metal.

was used not only to identify the phases in all samples, but also to calculate the volume fraction of retained austenite. The samples for analysis were mechanically ground and polished with 0.5-μm alumina powder to give the same surface conditions. A Rigaku Rotaflex anode X-ray diffractometer was interfaced with a computer to process the data. The samples were scanned from 30 to 110 deg with a step size of 0.02 deg. Each step size was allowed 50 s for X-ray detection. The integrated intensities were calculated using Philips XRD analysis software. The retained austenite content was calculated from the integrated intensities with a minimum of three austenite and three ferrite peaks and with the use of separation techniques where necessary.

Result and Discussion

Part A : Hydrogen Trapping in Austenite

Initial hydrogen thermal desorption was performed on atmospherically hydrogen-charged AISI type 304 stainless steel, which contains about 100 vol-% austenite. Figure 2 shows the thermal desorption for a wrought AISI type 304 stainless steel. Two hydrogen evolutions are noticeable, with the smaller one peaked at approximately 450°C. The predominant hydrogen evolution was observed to reach a peak at approximately 600°C and to cover a wide range of temperature (ΔT: temperature range between hydrogen evolution start and finish), from about 300°C up to 800°C (ΔT = 500°C). The predominant evolution peaked at approximately 600°C and covered a wide temperature range. It is possible that there are several defects (dislocations voids) and microconstituents in the austenite that acted as hydrogen trapping sites. At this point, the investigators did not attempt to precisely identify the origins of two distinctive evolutions, but rather intended to show that the two peaks are directly associated with the presence of austenite. Further investigations are necessary to resolve the two distinctive peaks. However, from an engineering standpoint, it is sufficient to know there is a strong entrapment of hydrogen by austenite. Hence, the predominant hydrogen evolution with 600°C peak temperature was a major focus because of its greater consequence on the welding of high-strength low-alloy steels.

The measured range of hydrogen evolution from thermal desorption analysis can be a quantitative indication of hydrogen transport or diffusion for this sample. This wide range of hydrogen evolution, as has also been predicted by Iino (Ref. 7), is due to the typical slow diffusivity and large solubility of hydrogen in austenitic microstructure.

The next sample for hydrogen thermal desorption analysis is super duplex stainless steels with a mixture of 50 vol-% austenite and 50 vol-% ferrite phase. Thermal desorption curve of the super duplex stainless steel sample is shown in Fig. 3. The result shows one broad hydrogen evolution with a peak at about 600°C. This result suggests hydrogen was released from the austenite (FCC) phase since hydrogen peak temperature appears to match with one for AISI type 304 stainless steel. This result implies that

Table 2 — Activation Energy for Hydrogen Release from Trap Sites

Trap Site	E_a (kJ/mol-H)	
H-Dislocation (mix)	26	(12)
H-Austenite bulk trap	55	
H-TiC interface	87	(13)

when both ferrite and austenite phases are present at the same time, most of the hydrogen trapping is controlled by the austenite phase. The temperature range of hydrogen evolution was observed from about 380 to 780°C (ΔT = 400°C). The SEM and TEM micrographs for the super duplex stainless steel are shown in Fig. 4. The white region in the SEM micrograph is ferrite phase and the darker region is austenite phase since the ferrite phase has more corrosion resistance against the etchant. The TEM micrograph for as-received super duplex stainless steel also shows the ferrite and austenite microstructure and the dislocations, which are primarily located in the austenite phase.

To investigate the transition of hydrogen behavior from stable austenite to unstable retained austenite, dual-phase steel was selected. The structure of dual-phase steels typically consists of a mixture of retained austenite, ferrite, and martensite. Thermal analysis was performed for gaseous-charged dual-phase steel, which was cold-rolled, intercritically annealed, and isothermally transformed sheet steels. Quantitative X-ray diffraction analysis revealed this process produced retained austenite typically in the amount of 12 vol-%. The thermal desorption shows two wide hydrogen evolution peaks, as shown in Fig. 5. Two evolution peaks were observed, which were 600°C and 680°C, respectively. The corresponding peak temperatures for the 12% retained austenite sample was 600°C. It is also apparent the lower peak temperature has the same peak temperature range with austenite intraphase trapping in the AISI type 304 stainless steel and super duplex stainless steel samples. The total temperature range for the two hydrogen evolutions is from about 480 to 770°C (ΔT = 250°C). In scanning electron micrographs, retained austenite appears smooth and has a brighter and featureless shape, leading to an easy distinction from ferrite and bainite as shown in Fig. 6 A and B. These micrographs prove the existence of retained austenite and show that most of the retained austenite was either located at the ferrite-austenite interfaces formed by intercritical annealing or surrounded by martensite (or bainite).

The following samples for the thermal

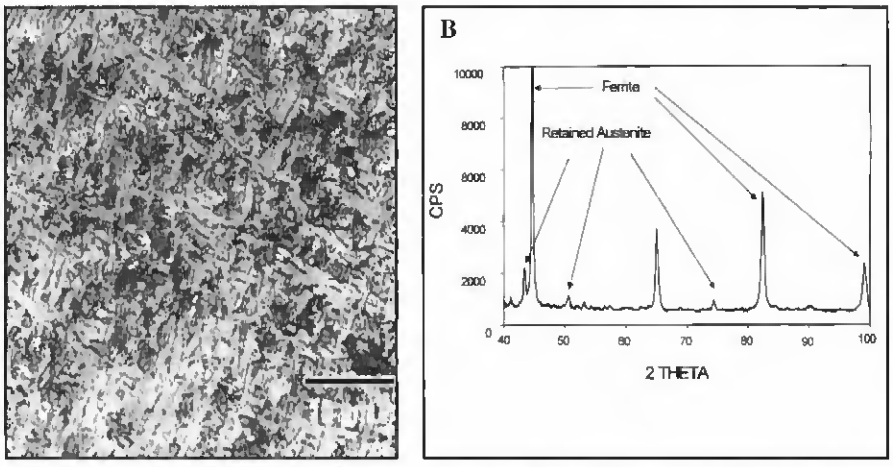

Fig. 8 — A — Optical microstructure of HSLA weld metal, which contains 4 vol-% retained austenite; B — X-ray analysis of HSLA steel weld metal, which contains 4 vol-% retained austenite.

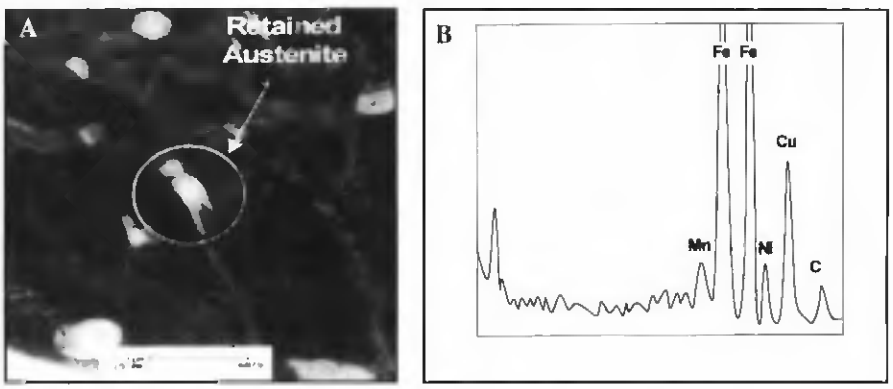

Fig. 9 — HSLA weld metal, which contains 4 vol-% retained austenite. A — TEM microstructure; B — EDS analysis on retained austenite particle.

desorption experiments are HSLA steel weld deposits. Due to the consequence of the welding cooling cycle, M-A constituents were produced in the weld deposit. Two different cooling processes were applied to generate a different amount of retained austenite: air cooling (4 vol-% retained austenite) and liquid nitrogen quenching (0 vol-% retained austenite). The thermal desorption results are shown in Fig. 7.

The hydrogen peak temperature for the air-cooled (4 vol-% retained austenite) sample was observed at 590°C, which is close to AISI type 304 stainless steel peak and super duplex stainless steel. The amount of hydrogen evolution is smaller than the previously analyzed three specimens. The hydrogen evolution temperature range was from about 520 to 690°C (ΔT = 170°C), suggesting a shorter distance for hydrogen to transport in migrating out of the retained austenite, compared to the AISI type 304 stainless steel sample. The high evolution peak temperature of the HSLA steel weld deposit sample also indicates that retained austenite, which is a consequence of welding cooling cycle, acts as a hydrogen trapping site.

The optical micrograph was obtained by using LePera's reagent (Refs. 8, 9), which was used to aid in differentiating the structures by tinting bainite as dark brown, ferrite as tan, and tempered martensite black. Retained austenite and untempered martensite are not affected by sodium metabisulfite and are left white. Figure 8A shows submicron-sized particles of retained austenite phase, shown as white and isolated islands, which can be easily distinguished from primary ferrite, ferrite with second phase, acicular ferrite, and tempered martensite. Figure 8B shows the X-ray diffraction analysis of the HSLA steel weld deposit, which has austenite peaks with a corresponding content of retained

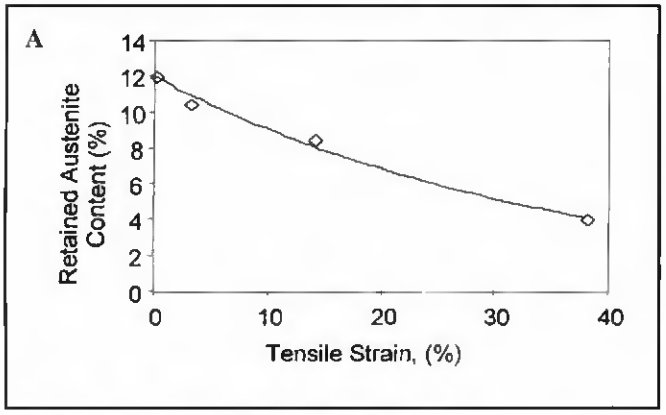

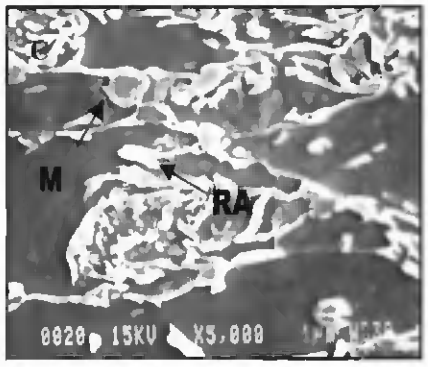

Fig. 10 — The measured retained austenite content. A — As function of tensile strain at room temperature; B — quenching temperature; C — scanning electron micrograph of steel structure deformed to a tensile strain of 10% at room temperature (M: martensite, RA: retained austenite).

austenite phase as much as 4%. The content of retained austenite phase was calculated from the X-ray diffraction pattern. TEM micrograph of retained austenite was also taken from the HSLA steel welded sample, which is shown in Fig. 9A. In the TEM micrograph, the retained austenite is located on the plate boundary. EDS analysis was carried out from scanning transmission electron microscopy (STEM) on the retained austenite particle. The EDS result, as shown in Fig. 9B, shows the retained austenite particle contains relatively high amounts of nickel, manganese, and copper elements, which are known as strong austenitic stabilizers.

Since the liquid-nitrogen-quenched weld deposit sample has almost zero volume percent of retained austenite, no high-temperature hydrogen peak was observed in Fig. 7. By comparing two thermal desorption curves, one can see the hydrogen is released from the liquid-nitrogen-quenched weld deposit at much lower temperature since this sample does not have a high-temperature hydrogen trap.

Hydrogen Trapping Characteristics of Retained Austenite

The retained austenite exhibited a high-peak temperature and a wide evolution temperature range as shown from thermal desorption analysis data for the 12% and 4% retained-austenite-containing specimens. The high-temperature hydrogen peak suggests that retained austenite is a strong trapping site. Further, the wide temperature range of hydrogen evolution indicates this microconstituent is an intraphase hydrogen trapping.

Quenching weld samples in liquid nitrogen is the common method to measure diffusible hydrogen since this practice can immobilize diffusible hydrogen under low-temperature conditions. While this practice is sufficient in quantifying the initial hydrogen contamination in the weld pool, it may mislead fabricators as to how safe the welding procedure is. Predictions for safe welding conditions, namely the P_{cm} method, utilize the measured diffusible hydrogen content to calculate the remaining content of diffusible hydrogen at the critical temperature (100°C). Such a prediction was developed by assuming 100% ferrite phase as the final transformation product, where hydrogen diffusivity is fast enough to enable sufficient hydrogen degassing. However, the presence of just a small volume fraction of retained austenite saturated with hydrogen may act as a barrier to hydrogen degassing and result in underestimation when using common, safe welding prediction methods.

On cooling, retained austenite is often the first to immobilize hydrogen in steel. With its sluggish hydrogen transport abilities, it retains the hydrogen down to low temperatures. Even with low-hydrogen pickup and high-quality welding procedures, it has likely immobilized most of the hydrogen. In this case, remaining hydrogen content at room temperature may be as high as the initial diffusible hydrogen, as measured by standard diffusible hydrogen measurement. With higher hydrogen pickup, retained austenite, depending on content, can become saturated with hydrogen, leaving the remaining hydrogen to be trapped by lower temperature traps or to stay as diffusible hydrogen.

It is common to apply different heating rates upon hydrogen thermal desorption to assess the trapping parameters of a trap site of interest. As the heating rate increased from 2 to 4°C per minute, the peak temperature, which corresponds to each trap site, increased. Using these data and Kissinger's equation (Equation 1), the activation energy for hydrogen release from the trap site (E_a) is obtained (Ref. 10).

$$\frac{\partial \ln\left(\phi / T_m^2\right)}{\partial\left(1/T_m\right)} = -\frac{E_a}{R} \quad (1)$$

where ϕ is the heating rate (K/min), T_m is the hydrogen evolution peak temperature, and R is the universal gas constant. E_a is the activation energy for hydrogen release from the trap site. According to this calculation, the activation energy for intraphase retained austenite trap is 55 kJ/mol-H. The trap activation energy is the sum of the trap-hydrogen binding energy (E_B) and the saddle point energy (E_S) ($E_a = E_B + E_S$). While the saddle point energy (E_S) should, in general, be any value less than E_a, some investigators assumed its value to be the same as the activation energy hydrogen diffusion in the matrix.

The activation energy for hydrogen release from the retained austenite phase is compared with those of other trapping sites, reported in a study by Lee, *et al.* (Refs. 12, 13), in Table 2. The capability of retained austenite to hold hydrogen atoms is shown to be stronger than dislocation (reversible trap), but weaker than TiC (irreversible trap). In this study, the investigators did not attempt to assess the binding energy value of retained austenite. Retained austenite trap sites would likely be satuated with hydrogen during

the course of the welding cooling cycle. Supersaturation, in this paper, is defined as a condition where the actual hydrogen concentration at retained austenite is higher than the equilibrium concentration determined by Silvert's law at ambient atmosphere condition. Therefore, E_a, which quantifies the hydrogen release process from retained austenite, is more useful information for safe welding predictions of HAC in steel welding.

At low temperatures, after welding, the release of hydrogen from the supersaturated retained austenite trap sites would take place very slowly due to the high value of E_a. In fact, the value of E_a measured in this study is only slightly higher than the reported value of activation energy for hydrogen diffusion in austenite lattice (E_L), which ranges from 41.6 to 54 kJ/mol (Ref. 11). With such a high E_a value, hydrogen diffusion from one site to another is almost impossible, especially at room temperature. Hence, it is possible that hydrogen atoms became permanently trapped in retained austenite lattice sites.

In this study, the investigators did not exclude the possibility of trap sites, such as dislocations, being present inside retained austenite. However, their presence might have been overshadowed by the lattice sites, which control the hydrogen release from retained austenite to a ferrite matrix. In addition, Lee, *et al.* (Ref. 14), suggested hydrogen transport behavior, including trapping and detrapping for FCC structured metals, is controlled by diffusion, and the trapping effects in interfacial trapping sites appear to be weak.

Part B: Retained Austenite Stability and the Distribution of Diffusible Hydrogen

Retained Austenite Stability

Retained austenite is known to transform to martensite with sufficient applied stress or with low service temperature. The retained austenite content for dual-phase steel, initially 12 vol-%, was measured both as a function of tensile strain at room temperature and quenching temperature. The resulting retained austenite contents are shown in Fig. 10A and B. The calculation of retained austenite contents for tensile strained samples was also done by XRD analysis. As the amount of tensile strain increased, the remaining retained austenite, which was not transformed to martensite, was decreased. This transformation is also known as stress-induced transformation. The critical strain required for transformation to martensite, however, might depend on several other factors, which control the stability of the retained austenite.

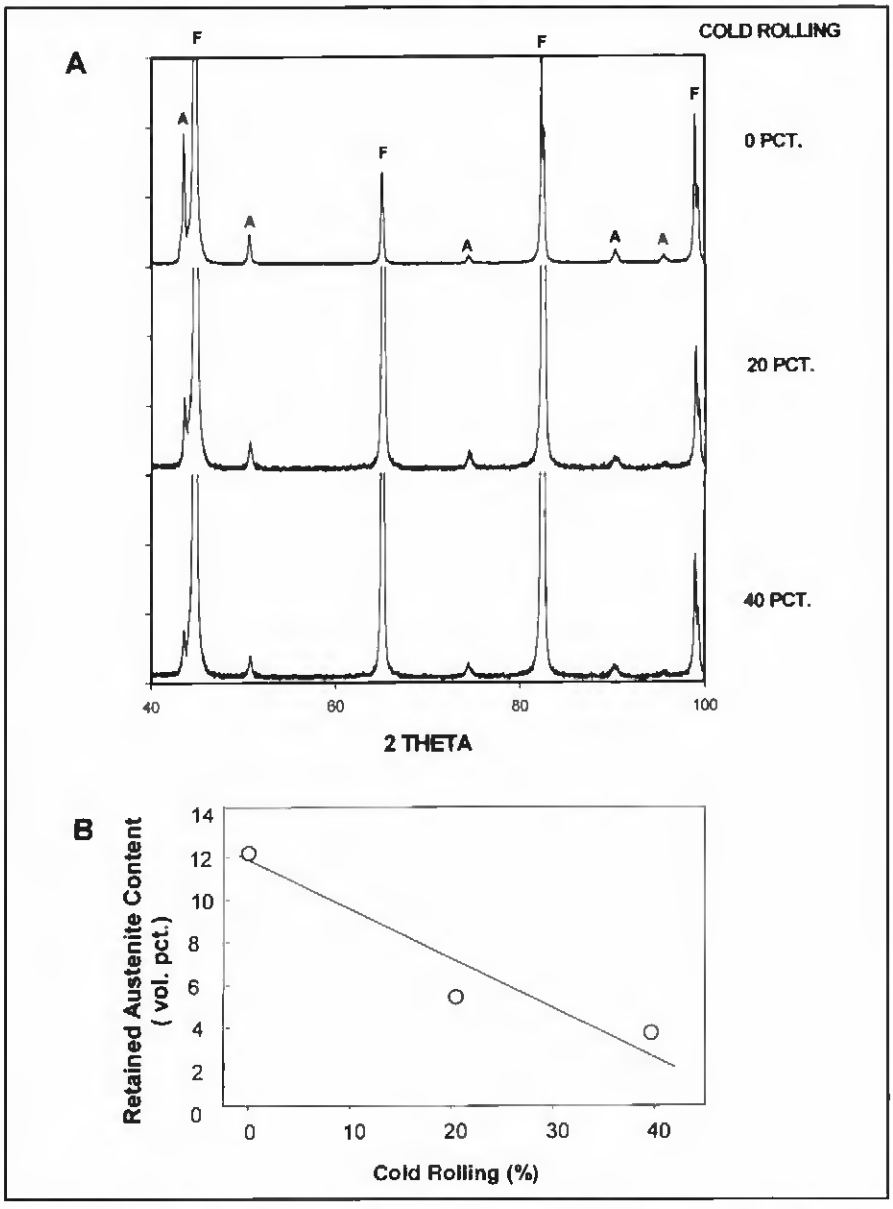

Fig. 11 — A — XRD result for 20 and 40% cold-rolled dual-phase steel (A — Austenite Peak and F — Ferrite Peak); B — the measured retained austenite content as function of cold rolling at room temperature.

The factors that can change stability include chemical composition, atomic size, and site and amount of deformation within the retained austenite. The other stability factor for retained austenite is temperature reduction since continuous cooling to subzero temperature promotes the transformation to martensite. The dual-phase steel was quenched in different cooling media, including dry ice-acetone solution and liquid nitrogen, to observe the transformation of retained austenite. The resulting retained austenite content is shown in Fig. 10B.

The scanning electron micrograph of Fig. 10C shows some indications of transformation from retained austenite to martensite. The microstructural constituent feature marked M represents martensite that was transformed from the retained austenite during tensile deformation and RA represents retained austenite. The retained austenite particles usually appear smooth and featureless, but martensite particles always revealed some substructure that might be a consequence of a stronger etching response.

Hydrogen Transport Model for Stress-Induced Retained Austenite

When hydrogen is trapped in retained austenite, a nonuniform distribution of hydrogen results due to the large differ-

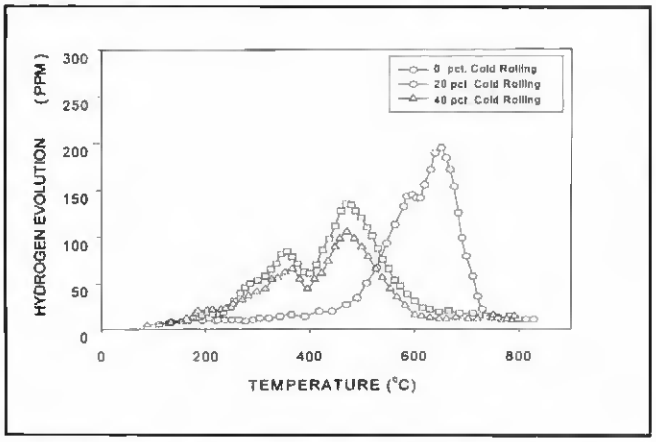

Fig. 12 — Thermal desorption analysis of stress-induced, dual-phase steel after gaseous hydrogen charging.

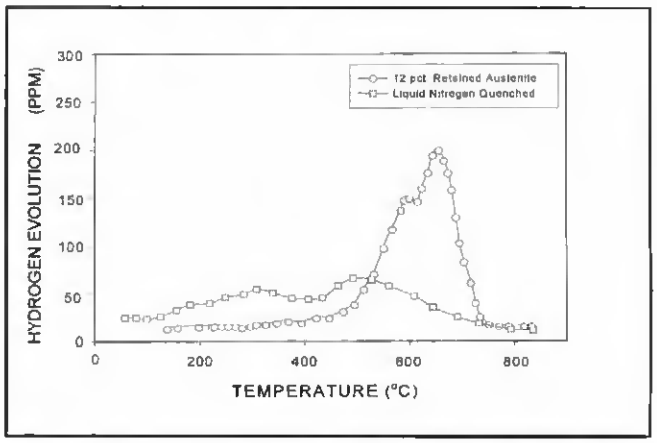

Fig. 13 — Thermal desorption analysis for dual-phase steel that is quenched in liquid nitrogen after charging.

ence in hydrogen solubility and diffusivity between ferrite and austenite. Once plastic strain is applied on the specimen and reaches a critical level, retained austenite transforms to martensite. This stress-induced transformation changes the hydrogen transport behavior due to the high diffusion rate and low solubility in the resulting martensite phase. In addition, this stress-induced transformation results in lowering the binding energy between the hydrogen and trapping site. This situation may have critical effects for hydrogen-assisted cracking (HAC) since hydrogen is sitting on the most susceptible microstructure and very likely diffuses to potential cracking sites.

The Effect of Retained Austenite Stability on Hydrogen Behavior in Dual-Phase Steels

Two stability factors, cold deformation and low-temperature quenching, were applied to observe the effect on hydrogen transport behavior. These two factors were selected to represent the possible service conditions, such as low service temperature and deformation. Since small amounts of retained austenite (about 4 vol-%) exist in HSLA steel weld deposits, dual-phase steels were used to observe the effect of retained austenite stability on hydrogen transport behavior.

XRD analysis was done for the 20 and 40% cold-rolled specimens to observe the respective changes in retained austenite content. XRD analysis results are shown in Fig. 11A. As the volume reduction of the sample increased by the cold rolling, the retained austenite content decreased as shown in Fig. 11B.

Thermal desorption analysis was performed for 20 and 40% cold-rolled, dual-phase steel specimens after gaseous hydrogen charging. The thermal desorptions shown in Fig. 12 indicate the hydrogen evolution peak was shifted to the lower temperature. This result shows clearer evidence of the alteration on the hydrogen trapping characteristic associated with retained austenite stability.

The effect of reduced temperature on hydrogen trapping behavior was also investigated. Liquid nitrogen was employed to transform the retained austenite to martensite for dual-phase steel that contains about 12 vol-% retained austenite. The specimen was quenched in liquid nitrogen after gaseous charging. Both the amount of hydrogen released from specimen and the hydrogen peak temperature were measured quantitatively with a constant heating rate (4°C/min) by using gas chromatography. Figure 13 shows the thermal analysis result for dual phase steel, which was quenched in liquid nitrogen after gaseous hydrogen charging. Almost the same hydrogen evolution profile was observed in these specimens as for cold-rolled specimens with thermal desorption analysis. This observation suggests lowering the temperature has a similar influence on hydrogen behavior compared with deformation due to the transformation of retained austenite.

Engineering and Commercial Importance

Hydrogen trapping in retained austenite, if not properly understood and managed, can be a critical factor for HAC in HSLA steel weldments. In commercial applications, retained austenite transformation to martensite can occur when HSLA steel weldments are used in structures under severe cold conditions or with localized weld deformation, possibly due to residual stresses.

Conclusions

1) Retained austenite in high-strength steel welds is a significant high-temperature bulk hydrogen trap that must be considered in the determination of hydrogen cracking susceptibility.

2) Hydrogen trapping by retained austenite is associated with a very slow hydrogen transport with the austenite phase and is not a hydrogen-interface interaction. At low temperature, even austenite lattice sites behave as trap sites because there is not sufficient thermal energy for the hydrogen atoms to overcome the energy harrier for hydrogen diffusion in an austenite lattice.

3) The existence of retained austenite means an underestimation of the amount of remaining diffusible hydrogen, when calculated based on standard diffusible hydrogen measurement. As a consequence, common methods to predict safe welding conditions from HAC become too optimistic.

4) By applying different amounts of plastic strains, the retained austenite transforms to martensite and alters the hydrogen detrapping behavior.

5) Quenching to liquid nitrogen temperature eliminates the existence of the retained austenite and no significant high temperature peak for hydrogen trapping was found.

Acknowledgment

The authors acknowledge and appreciate the research support of the United States Army Research Office.

References

1. Yurioka, N., and Suzuki, H. 1990. Hydrogen assisted cracking in C-Mn and low alloy

steel weldments. *International Materials Review* 35(4): 217–249.

2. Maroef, I., Olson, D. L., Eberhart, M., Edwards, G. R., and Lensing, C. 2000. Weld metal hydrogen trapping. Submitted to *International Metallurgical Review*, Colorado School of Mines, Golden, Colo.

3. Maroef, I. S., and Olson, D. L. 2000. Fundamental aspects of hydrogen trapping in steel weld metal. *Proc. Joining of Advanced and Specialty Materials II*, pp. 227–235, ASM International, Materials Park, Ohio.

4. Pressouyre, G. M., and Bernstein I. M. 1981. An example of the effect of hydrogen trapping on hydrogen embrittlement. *Met. Trans. A* 12A(5): 835–844.

5. Wildash, C., Cochrane, R. C., Gee, R., and Widgery, D. J. 1998. Microstructural factors affecting hydrogen induced cold cracking in high strength steel weld metal. *Proc. 5th International Conference, Trends in Welding Research*, pp. 745–750. ASM International, Materials Park, Ohio.

6. Nelson, H. G. 1983. Hydrogen embrittlement. Treatise on materials science and technology, 25. *Embrittlement of Engineering Alloys*. eds. C. L. Briant, S. K. Banerji, pp. 275–395. Academic Press, Inc.

7. Iino, M. 1998. Evaluation of hydrogen-trap binding enthalpy II. *Met. Trans.* 29A: 1017–1021.

8. LePera, F. S. 1980. Improved etching technique to emphasize martensite and bainite in high-strength dual-phase steel. *J. Met.* 32(3): 38–39.

9. LePera, F. S. 1979. Improved etching technique for the determination of percent martensite in high-strength dual-phase steels. *Metallography* 12: 263–268.

10. Kissinger, H. E. 1957. Reaction kinetics in differential thermal analysis. *Analytical Chemistry* 29: 1702–1706.

11. Bollinghaus, T., Hoffmeister, H., and Middel, C. 1996. Scatterbands for hydrogen diffusion coefficients in steels having a ferritic or martensitic microstructure and steels having an austenitic microstructure at room temperature. *Welding in the World* 37(1): 16–23.

12. Lee, H. G., and Lee, J. Y. 1984. Hydrogen trapping by TiC particles in iron. *Acta Metall.* 32(1): 131–136.

13. Choo, W. Y., and Lee, J. Y. 1982. Thermal analysis of trapped hydrogen in pure iron. *Metall. Trans.* A. 13A: 135–140.

14. Lee, J. Y., and Lee, S. M. 1986. Hydrogen trapping phenomena in metals with B.C.C. and F.C.C. crystal structures by the desorption thermal analysis technique. *Surface and Coating Technology* 28: 301–314.

Preparation of Manuscripts for Submission to the *Welding Journal* Research Supplement

All authors should address themselves to the following questions when writing papers for submission to the Welding Research Supplement:

- Why was the work done?
- What was done?
- What was found?
- What is the significance of your results?
- What are your most important conclusions?

With those questions in mind, most authors can logically organize their material along the following lines, using suitable headings and subheadings to divide the paper.

1) **Abstract.** A concise summary of the major elements of the presentation, not exceeding 200 words, to help the reader decide if the information is for him or her.

2) **Introduction.** A short statement giving relevant background, purpose and scope to help orient the reader. Do not duplicate the abstract.

3) **Experimental Procedure, Materials, Equipment.**

4) **Results, Discussion.** The facts or data obtained and their evaluation.

5) **Conclusion.** An evaluation and interpretation of your results. Most often, this is what the readers remember.

6) **Acknowledgment, References and Appendix.**

Keep in mind that proper use of terms, abbreviations and symbols are important considerations in processing a manuscript for publication. For welding terminology, the *Welding Journal* adheres to ANSI/AWS A3.0-94, *Standard Welding Terms and Definitions.*

Papers submitted for consideration in the Welding Research Supplement are required to undergo Peer Review before acceptance for publication. Submit an original and one copy (double-spaced, with 1-in. margins on 8 ½ x 11-in. or A4 paper) of the manuscript. Submit the abstract only on a computer disk. The preferred format is from any Macintosh® word processor on a 3.5-in. double- or high-density disk. Other acceptable formats include ASCII text, Windows™ or DOS. A manuscript submission form should accompany the manuscript.

Tables and figures should be separate from the manuscript copy and only high-quality figures will be published. Figures should be original line art or glossy photos. Special instructions are required if figures are submitted by electronic means. To receive complete instructions and the manuscript submission form, please contact the Peer Review Coordinator, Doreen Kubish, at (305) 443-9353, ext. 275; FAX (305) 443-7404; or write to the American Welding Society, 550 NW LeJeune Rd., Miami, FL 33126.